A&A 487, L21–L24 (2008)
DOI: 10.1051/0004-6361:200810217

Astronomy & Astrophysics

Letter to the Editor

Ion reflections from the parallel MHD termination shock and a possible injection mechanism into the Fermi-1 acceleration

H.-J. Fahr and D. Verscharen

Argelander Institute for Astronomy, University of Bonn, Auf dem Hügel 71, 53121 Bonn, Germany
e-mail: dverscha@astro.uni-bonn.de

Received 19 May 2008 / Accepted 17 June 2008

ABSTRACT

Context. The analysis with our recently developed kinetic solar wind termination shock model for a parallel magnetic field orientation has shown several interesting features of the ion distribution function at the downstream side of the magnetohydrodynamic shock. Among these results, it turned out that a certain amount of ions are provided with a velocity backwards into the shock transition layer by turbulent interaction.

Aims. The behaviour of these reflected ions during their second shock transit towards the upstream side is investigated. The reflected particles become an additional ion species in the foreshock region, and their influence on the upstream plasma environment has to be studied and evaluated.

Methods. Under the same shock conditions as adopted in our first paper, we treated these reflected ions kinetically with the methods of our model to solve the appropriate Boltzmann-Vlasov equation. The modified transport equation was solved with the help of stochastic differential equations.

Results. The shock scenario leads to fast ion beams oriented backwards into the foreshock region. About 18% of the incoming solar wind ions are reflected and affect the upstream plasma flow. With these properties the treated processes clearly indicate an additional injection mechanism for ACRs.

Key words. plasmas – shock waves – magnetohydrodynamics (MHD) – acceleration of particles

1. Introduction

MHD shocks are proven to have some limited efficiency in reflecting particles back into the upstream direction and therefore operate as ion injectors into an ongoing Fermi-1 acceleration process (Pesses et al. 1981; Potgieter & Moraal 1988; Jokipii 1992; Donohue & Zank 1993; Chalov & Fahr 1994, 1995). The necessary reflection mechanisms have already been investigated in more detail for the case of quasi-perpendicular shocks where adiabatic or mirror reflections can be shown to be responsible for reflecting specific ions out of the upstream velocity distribution function (see Chalov & Fahr 1996, 2000). The reflection conditions (see Decker 1988) are thus very sensitive to the local angle θ_{Bn} between the upstream interplanetary magnetic field and the shock normal (Chalov 1993; Chalov & Fahr 1996; Schwadron & McComas 2003; Kucharek & Scholer 1995; Chalov 2005; Meziane et al. 2005).

On the other hand, an adequate description of the microphysical processes enforcing ion reflections is harder to provide for the parallel MHD shock due to the lack of changes in the shocked quiet magnetic field in this case. An adequate description may only be derivable from a detailed kinetic study. In this paper we thus want to come back to our recent results in kinetically modelling the quasiparallel MHD shock and, by integration of the Boltzmann-Vlasov equation over the termination shock, providing the downstream ion distribution function (Verscharen & Fahr 2008). In this theoretical approach we have described the change in the ion distribution function at the ion passage over the shock transition region taking conservative actions of static and stochastic actions of turbulent shock-electric fields into account. One can see from this result that a doubly-humped ion distribution evolves on the downstream side which contains ions in the negative velocity branch. The latter ones tend to again run back into the shock structure and are subject to further phasespace processings there under the influence of the electric field and electrostatic turbulences excited by the over-shooting electrons. Under these conditions, the retrograde ions are now accelerated by the field into the upstream direction and, additionally, a further dissipative broadening of the distribution function is expected with the probability of a change of the direction of motion (the re-reflected ions). The reflected particles are likely to become potential candidates for ions which finally become ejected from the shock into the upstream regime. In the following we study the dynamics of these identified reflected downstream ions in kinetic detail to find the phasespace properties of such ions in the state where they are eventually reflected from the shock into the upstream regime.

There are several observations, especially from the foreshock region at the earth bow shock, that show reflected solar wind particles (Meziane et al. 2005). The main characteristics of these so-called field-aligned beams (FAB) are high velocities in the range of the upstream solar wind speed and high temperatures in the range of several 10^6 K (Paschmann et al. 1981). CLUSTER observations show a strong dependence of these ion beams on the magnetic field orientation, characterised by the angle between the local shock normal and the direction of the magnetic field θ_{Bn} (Meziane et al. 2007). Up to now the reflection mechanisms have not been completely understood. From a rather extrinsic point of view, the reflection can be handled with the help of

Article published by EDP Sciences

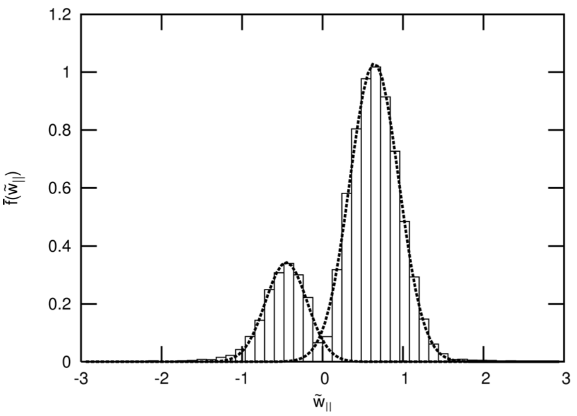

Fig. 1. Normalised ion distribution function on the downstream side of the solar wind termination shock. The velocity $\tilde{w}_{\|}$ is normalised to the upstream ion bulk velocity. The dotted curves are fit results.

conservation laws (Paschmann et al. 1980), but the acting processes and the cause for the appearance of the reflected ions are essentially not known. Furthermore, there are perhaps already observational hints available for the existence of shock-reflected ions in the precursor region of the solar wind termination shock. On Dec. 16, 2004, VOYAGER-1 was claimed to have crossed the termination shock at a distance of 94 AU (see Fisk 2005). There have, however, been striking precursor events in the region ahead of the shock before this crossing event. For example there were a series of increases in the intensity of low-energy ions connected with strong anisotropies and ion-fluxes coming from antisolar directions, and these phenomena gave rise to controversely speculate on a possible shock crossing already in Dec. 2003 (see Krimigis et al. 2003; McDonald et al. 2003; Burlaga et al. 2003). The surprising phenomena seen by the VOYAGER-1 detectors in this phase could well have been connected with ions reflected from the shock into the upstream solar wind region.

2. The reflected ions in our model

From our recent model calculations (Verscharen & Fahr 2008), it turns out that, because of stochastic interaction processes with electrostatic turbulences within the shock transition, a non-negligible fraction of ions appears on the downstream side of the shock within the negative branch of the ion velocity distribution function; i.e., this fraction represents an ion population with "negative" individual velocities $w_{\|}$. An example of the normalised downstream ion distribution function for calculations by the model under a typical parameter choice for the quiet solar wind (cf. Marsch 2000) is shown in Fig. 1.

These ions have to be treated with special care within our kinetic theory. At first glance, an individual ion should not be able to reach the downstream side of the shock region, if somewhere within the transition region it has attained a negative velocity, i.e. one directed into the upstream direction. Nevertheless the occurrence of reflected ions on the downstream side does not indicate an inconsistency in the solution within our kinetic treatment, but simply expresses that some ions arriving downstream with low or vanishing positive velocities due to ongoing stochastic interaction processes finally attain negative velocities again. In contrast, there is good reason to take these upstream flowing ions as serious input for further kinetic treatment leading towards the better asymptotic consistency not yet achieved in our earlier approach (Verscharen & Fahr 2008), as we are going to show. Neither in the upstream nor in the downstream region does the ion distribution function undergo any changes within our Boltzmann-Vlasov treatment; it does, however, change its profile exclusively in the transition region of the shock layer. At large distances from the shock, where $U(s)$ is constant and no turbulent interaction occurs (n.b.: $D_{\|}(s) \approx 0$) ions propagate without any changes in their kinetic characteristics. This means that the resulting downstream distribution function reflects the enduring downstream ion phasespace conditions. There will be some ions that already attain a "negative" velocity $w_{\|}$ soon after entrance into the transition region and thus do not carry out a full shock passage. The fraction of such early reflected ions is fairly low, since the strength of the stochastic interaction grows with each step ds in the downstream direction. This can be revealed easily by inspection of different paths of the underlying Wiener process (see Verscharen & Fahr 2008), where velocity differences (averaged over many paths) grow with the increasing duration of the stochastic process. Thus, a particle has to penetrate deeply into the transition region, until it is finally reversed to a negative velocity. This means that, although the branch with negative ion velocities $w_{\|}$ appears in a first view as a numerical artefact, it deserves in fact to be taken serious as the basis of an appropriate estimation for ion reflections at the shock. Thus in the following, we study the evolution of the negative velocity branch of the ion distribution, advancing the integration of the Boltzmann-Vlasov equation from the downstream to the upstream side of the shock.

Table 1. Fit results and their physical interpretation.

Parameter	Value	Physical interpretation
$a_{\rm r}$	1.394 ± 0.011	
$b_{\rm r}$	8.74 ± 0.15	$\Rightarrow T_1^{\rm refl} = 1.1 \times 10^6$ K
$c_{\rm r}$	-1.1519 ± 0.0022	$\Rightarrow U_1^{\rm refl} = -4.6 \times 10^7$ cm s^{-1}
$b_{\rm rr}$	12.05 ± 0.97	$\Rightarrow T_{1,\rm rr}^{\rm refl} = 8.0 \times 10^5$ K
$c_{\rm rr}$	1.0554 ± 0.0089	$\Rightarrow U_{1,\rm rr}^{\rm refl} = 4.2 \times 10^7$ cm s^{-1}

The downstream ion distribution function is taken as a Maxwellian profile with the parameters from the fit in Verscharen & Fahr (2008). It is centred at $U_2^{\rm refl}$ with $T_2^{\rm refl} = 1.24 \times 10^5$ K. The negative bulk velocity of the reflected ions is obtained as $U_2^{\rm refl} = -1.8 \times 10^7$ cm s^{-1}. The negative sign indicates the direction towards the inner heliosphere. These fit parameters depend almost solely on the shock thickness. The greater the thickness, the higher the absolute value of $U_2^{\rm refl}$ and the temperature. The relative percentage of reflected ions is determined by evaluating the integral

$$\int_{-\infty}^{0} \bar{f}(\tilde{w}_{\|}) \mathrm{d}\tilde{w}_{\|} = \int_{-\infty}^{0} 0.343 \cdot \mathrm{e}^{-7.5(\tilde{w}_{\|}+0.45)^2} \mathrm{d}\tilde{w}_{\|} = 0.22, \tag{1}$$

which means that 22% of the upstream ions are reflected, whereas 78% propagate into the heliosheath and the interstellar space ($\bar{f}$ is normalised to 1). An error margin for this amount can be estimated by integrating the distribution for the limits given by the errors in Table 1 in Verscharen & Fahr (2008). A difference of ±0.01 for the amount of reflected ions occurs within this margin. The unreflected ions (with positive individual velocities on the downstream side) are excluded from the upcoming considerations. With that understanding, the distribution function of reflected ions can now be normalised again to 1.

3. Incorporation of the reflected ions into our model

For this study the main properties of the shock are kept identical to those derived in our previous model (Verscharen & Fahr 2008). This implies an initial electric field $\mathcal{E}$ acting in the shock structure given by

$$\mathcal{E} \approx \frac{m_\mathrm{p}}{e} U \frac{\mathrm{d}U}{\mathrm{d}s} = \frac{m_\mathrm{p}}{2e} \frac{\mathrm{d}U^2}{\mathrm{d}s} \cdot \tag{2}$$

Here $U(s)$ is the bulk velocity profile of the ion flow describing a drop from U_1 on the upstream side (where the space coordinate s is negative) down to $U_2 = U_1/r$ on the downstream side ($s > 0$). Here r denotes the compression ratio, which had been calculated as 2.5. As before, the bulk velocity profile is parametrised by

$$U(s) = \frac{U_1 + U_2}{2} - \frac{U_1 - U_2}{2} \cdot \tanh\left(\frac{s}{\lambda}\right). \tag{3}$$

This means that the decelerating field is still dominated by the bulk velocity profile $U(s)$ of the ions and the diffusion by the bulk velocity profile $u_\mathrm{e}(s)$ of the electrons. The profiles of the electron flow from upstream to downstream are given further on by the same system as before:

$$u_\mathrm{e}(s) = u_\mathrm{e}^\mathrm{el}(s) + u_\mathrm{e}^\mathrm{turb}(s) \tag{4}$$

$$u_\mathrm{e}^\mathrm{el} = \sqrt{\frac{m_\mathrm{p}}{m_\mathrm{e}}} U \sqrt{\frac{U_1^2}{U^2}\left(1 + \frac{m_\mathrm{e}}{m_\mathrm{p}}\right) - 1} \tag{5}$$

$$u_\mathrm{e}^\mathrm{turb}(s) = \frac{U_2 - u_{\mathrm{e},2}^\mathrm{el}}{2} + \frac{U_2 - u_{\mathrm{e},2}^\mathrm{el}}{2} \cdot \tanh\left(\frac{s-b}{\mu}\right). \tag{6}$$

The diffusion coefficient still depends on the difference between ion and electron bulk velocities. The electron flow is assumed to be given by the same $u_\mathrm{e}(s)$ as determined in the earlier calculations. The ion bulk velocity must be obtained as the first moment of the reflected ion distribution function:

$$U^\mathrm{refl}(s) = \frac{1}{N} \int_{-\infty}^{+\infty} w_\parallel f^\mathrm{refl}(w_\parallel, s) \mathrm{d}w_\parallel. \tag{7}$$

Therefore, it becomes necessary to evaluate $f^\mathrm{refl}(w_\parallel, s)$ at every step s, which is on the one hand a more laborious numerical work but, on the other hand, provides important additional information about the ion behaviour. The diffusion coefficient is then given by

$$D_\parallel^\mathrm{refl} = \frac{\sqrt[3]{\frac{4m_\mathrm{p}}{m_\mathrm{e}}}}{\sqrt{3}} \left(\frac{m_\mathrm{e}}{m_\mathrm{p}}\right)^2 \omega_\mathrm{p} \left(u_\mathrm{e} - U^\mathrm{refl}\right)^2. \tag{8}$$

With these expressions, the new transport equation can be specified:

$$\frac{\partial f^\mathrm{refl}}{\partial s} = -\frac{1}{2} \frac{\mathrm{d}U^2(s)}{\mathrm{d}s} \frac{1}{w_\parallel} \frac{\partial f^\mathrm{refl}}{\partial w_\parallel} + \frac{1}{w_\parallel} D_\parallel^\mathrm{refl} \frac{\partial^2 f^\mathrm{refl}}{\partial w_\parallel^2} \cdot \tag{9}$$

The ion distribution function is re-normalised to one. Corresponding to (9), one finds the stochastic differential equation

$$\mathrm{d}w_\parallel = \frac{1}{2} \frac{\mathrm{d}U^2(s)}{\mathrm{d}s} \frac{1}{w_\parallel} \mathrm{d}s + \sqrt{\frac{2D_\parallel^\mathrm{refl}}{|w_\parallel|}} \mathrm{d}W_s \tag{10}$$

with $\mathrm{d}s = w_\parallel \mathrm{d}t$. One should note here that the first term (the drift term) does *not* contain the bulk velocity $U^\mathrm{refl}(s)$ of the reflected ions. This assures that the electric potential is still dominated by the plasma flow from upstream to downstream.

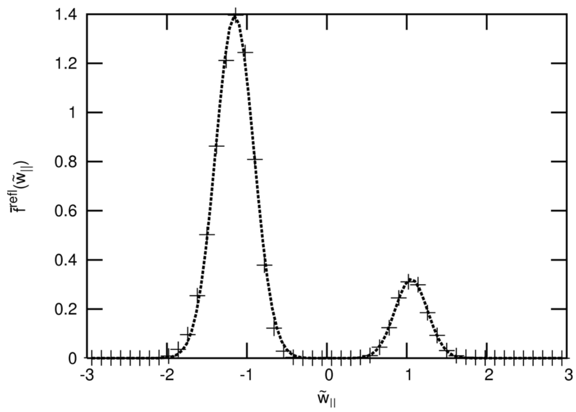

Fig. 2. Normalised ion distribution function on the upstream side of the shock for the reflected ions. Again, as expected, a new double-hump structure has built up. The dotted curves are fit results.

4. Results and discussion

The stochastic differential Eq. (10) is evaluated with the same parameters as in the earlier model, however, starting with the distribution f^refl of reflected ions at the downstream boundary of the shock transition region. The resulting distribution function on the upstream boundary is shown in Fig. 2.

Evidently, a new double-hump structure has built up for the reflected ions. This means that a certain number of ions (hereafter called "re-reflected ions") have changed direction for a second time and move now towards the downstream direction. The other part (the left beam) has a rather high velocity and a comparatively high temperature in contrast to the environment of the upstream solar wind plasma.

Two Gaussian profiles of the form

$$\begin{aligned} \bar{f}^\mathrm{refl} &= \left[\bar{f}_\mathrm{r}(\tilde{w}_\parallel)\right] + \left[\bar{f}_\mathrm{rr}(\tilde{w}_\parallel)\right] &(11)\\ &= \left[a_\mathrm{r} \cdot \mathrm{e}^{-b_\mathrm{r}(\tilde{w}_\parallel - c_\mathrm{r})^2}\right] + \left[\left(\sqrt{\frac{b_\mathrm{rr}}{\pi}} - \sqrt{\frac{b_\mathrm{rr}}{b_\mathrm{r}}} a_\mathrm{r}\right) \cdot \mathrm{e}^{-b_\mathrm{rr}(\tilde{w}_\parallel - c_\mathrm{rr})^2}\right] &(12) \end{aligned}$$

are a fitting description for the reflected distribution. The fit result is shown in Table 1.

The fit can again be used to determine the ratio of reflected and re-reflected ions. Integrating $\bar{f}_\mathrm{r}$ from Eq. (11) yields that the percentage of ions, which are reflected into the upstream direction, amounts to 84% of the initially backwards directed ions, which means that 16% are re-reflected and can undergo another shock transition. Considering that only 22% get negative velocities at their first shock transition, one finds that, in total balance, $p_\mathrm{r} = 0.22 \times 0.84 = 0.18 \mathrel{\hat{=}} 18\%$ of the solar wind ions are in fact reflected; i.e., $p_\mathrm{t} = 1 - 0.18 = 0.82 \mathrel{\hat{=}} 82\%$ propagate totally into the heliosheath. Because the momenta of the final distribution function depend almost exclusively on the shock thickness, the latter represents the crucial parameter. As mentioned before, a larger thickness would lead to both a higher bulk velocity and a higher temperature after shock transit. Additionally, it would yield an increase in the reflected ion fraction. If the parameters are chosen within the limits of the usual conditions for the quiet solar wind, the result is only weakly sensitive to them. Similar to the requirements from the Rankine-Hugoniot conditions, one can use the mass conservation as a possible way to determine the particle density of the participating particle populations. For this purpose the shock can be treated like a box with a total mass inflow from the upstream side and an outflow to both the upstream (reflected ions) and the downstream (propagating ions) directions. Obviously for the sake of stationarity, the total inflow must be balanced by the total outflow ($n_1 U_1 = n_t U_t + n_r U_r$). All velocities are taken as their particular absolute value. The particle outflow occurs with the same ratio as the involved beam particle amounts. This means that $(n_t U_t / n_r U_r) = (p_t / p_r)$ provides a way to express the reflected particle density in the dependence of the upstream conditions:

$$n_r = \frac{n_1 U_1}{U_r} \cdot \frac{1}{\frac{p_t}{p_r} + 1} \cdot \tag{13}$$

In our special situation this leads to a density of the reflected ions of $n_r = 8 \times 10^{-5}\,\mathrm{cm}^{-3}$. This immediately offers the opportunity to calculate the density of the propagating particles to $n_t = 4 \times 10^{-4}\,\mathrm{cm}^{-3}$.

5. Conclusions

The main result of our considerations is that we can prove that hot and fast reflected ions are reappearing in the upstream flow regime. About 18% of the original solar wind ions coming from the upstream side undergo a reflection at the parallel shock in this way. On first view, one could expect a strictly ongoing broadening of the distribution function due to turbulent interaction because the diffusion coefficient (8) never reaches a value of zero. In contrast to the primary model calculations, the ions and electrons do not reach the same bulk velocity in this case, which is inherently given by their oppositely directed motions. However, we find that the bulk velocity difference $u_e - U^{\mathrm{refl}}$ (also the square of the difference) is for a sufficient distance from the shock region negligibly small for a sufficient distance from the shock region compared to its value during over-shooting. Hence, the stream situation on the upstream side is slightly unstable, but this instability is not able to excite heavy electrostatic turbulence. Presumably, other processes as pitch-angle diffusion would annihilate the reflected beam shape on smaller time scales than the turbulent electrostatic wave-particle interaction.

The particle density of the reflected ions is rather high. Totally, about 1/7 of the upstream ion population near the shock consists of reflected ions ($n_r = 8 \times 10^{-5}\,\mathrm{cm}^{-3}$). In comparison to the other particle populations at the upstream side, this value shows that the number of the reflected ions is not negligible for an appreciable description of the foreshock regime. For comparison, the pick-up ion density there amounts to about $2.1 \times 10^{-4}\,\mathrm{cm}^{-3}$ (Fisk et al. 2006).

Space probe measurements of reflected ions at the earth's bow shock find particle densities of about 13% of the incident solar wind densities (Paschmann et al. 1981), which accords well with our value (16%), even though the conditions differ between the two shock situations. Also at the earth bow shock, the reflected ions show high bulk velocities and high temperatures. Typically, the beam temperatures are around several times 10^6 K and the bulk velocity ranges from one to five times the solar wind bulk velocity. Of course the remarks on the meaning of the reflected distribution function given in Sect. 2 are also valid for the re-reflected ions. These are the ions that now have a *positive* value for $w_\parallel$ and are therefore again reversed back into the downstream direction.

It is now appropriate to discuss the fate of these shock-reflected ions within a consistent picture of processes determining the complicatedly entangled wave-plasma physics in the upstream precursor and the transition region of the termination shock. As shown above, the reflected ions enter the upstream region with velocities near the solar wind velocity with respect to the shock frame. They are, however, directed opposite to the solar wind flow direction, and hence are seen by the solar wind bulk with about twice the solar wind velocity. Since the solar wind carries with it co-convected and ion-selfgenerated magnetoacoustic turbulences (see Chashei et al. 2003; Chalov et al. 2004, 2006), these shock-reflected ions undergo pitch-angle scattering by wave-plasma interactions with these turbulences (see e.g. Chashei et al. 2003; Chashei & Fahr 2005). The longer these reflected ions undergo those scattering processes, the more they are redistributed into a pitch-angle isotropic distribution function in which all of these ions are re-populated into a spherical shell in velocity space centred at the upstream solar wind bulk velocity with a shell radius of about twice the solar wind bulk velocity.

As can be expected from that scenario all the shock-reflected ions eventually are convected back into the shock structure sitting, however, at this time in this extended, energised, wind-convected shell. It is fairly evident that a high percentage of these shell ions are deposited in a region of velocity space that does not allow them to overcome the shock-electric potential well. Thus, these ions are permanently undergoing reflections at this well and thereby naturally enter into the Fermi-1 acceleration process from which the anomalous cosmic ray ions are created (see Chalov & Fahr 1994, 1995; le Roux & Fichtner 1997; Scherer et al. 1998). In a forthcoming paper we shall study the fate of these isotropised, shock-reflected ions when they are again re-convected into the shock structure.

Acknowledgements. The authors are grateful to the Deutsche Forschungsgemeinschaft for financial support within the frame of the DFG project Fa 97/31-2.

References

Burlaga, L. F., Ness, N. F., Stone, E. C., et al. 2003, Geophys. Res. Lett., 30, 9
Chalov, S. 1993, Adv. Sp. Res., 13, 293
Chalov, S. V. 2005, Adv. Sp. Res., 35, 2106
Chalov, S. V., & Fahr, H. J. 1994, A&A, 288, 973
Chalov, S. V., & Fahr, H. J. 1995, Planet. Space Sci., 43, 1035
Chalov, S. V., & Fahr, H. J. 1996, Sol. Phys., 168, 389
Chalov, S. V., & Fahr, H. J. 2000, A&A, 360, 381
Chalov, S. V., Alexashov, D. B., & Fahr, H. J. 2004, A&A, 416, L31
Chalov, S. V., Alexashov, D. B., & Fahr, H. J. 2006, Astr. Lett., 32, 206
Chashei, I. V., & Fahr, H. J. 2005, Adv. Sp. Res., 35, 2078
Chashei, I. V., Fahr, H. J., & Lay, G. 2003, Ann. Geo., 21, 1405
Decker, R. B. 1988, Sp. Sci. Rev., 48, 195
Donohue, D. J., & Zank, G. P. 1993, J. Geophys. Res., 98, 19005
Fisk, L. A. 2005, Science, 309, 2016
Fisk, L. A., Gloeckler, G., & Zurbuchen, T. H. 2006, ApJ, 644, 631
Jokipii, J. R. 1992, ApJ, 393, L41
Krimigis, S. M., Decker, R. B., Hill, M. E., et al. 2003, Nature, 426, 45
Kucharek, H., & Scholer, M. 1995, J. Geophys. Res., 100, 1745
le Roux, J. A., & Fichtner, H. 1997, J. Geophys. Res., 102, 17365
Marsch, E. 2000, in The Outer Heliosphere: Beyond the Planets, ed. K. Scherer, H. Fichtner, & E. Marsch, 41
McDonald, F. B., Stone, E. C., Cummings, A. C., et al. 2003, Nature, 426, 48
Meziane, K., Wilber, M., Mazelle, C., Parks, G. K., & Hamza, A. M. 2005, in The Physics of Collisionless Shocks: 4th Annual IGPP Inter. Astrophys. Conf., ed. G. Li, G. P. Zank, & C. T. Russell, AIP Conf. Ser., 781, 116
Meziane, K., Wilber, M., Hamza, A. M., et al. 2007, J. Geophys. Res., 112, 1101
Paschmann, G., Sckopke, N., Asbridge, J. R., Bame, S. J., & Gosling, J. T. 1980, J. Geophys. Res., 85, 4689
Paschmann, G., Sckopke, N., Papamastorakis, I., et al. 1981, J. Geophys. Res., 86, 4355
Pesses, M. E., Eichler, D., & Jokippi, J. R. 1981, ApJ, 246, L85
Potgieter, M. S., & Moraal, H. 1988, ApJ, 330, 445
Scherer, K., Fichtner, H., & Fahr, H. J. 1998, J. Geophys. Res., 103, 2105
Schwadron, N. A., & McComas, D. J. 2003, Geophys. Res. Lett., 30, 41
Verscharen, D., & Fahr, H.-J. 2008, A&A, 487, 723